
Learning stochastic multiscale models through normalizing flows ^{*}

Anan Saha

Department of Mathematics
Louisiana State University
Baton Rouge, LA 70802
asaha9@lsu.edu

Arnab Ganguly [†]

Department of Mathematics
Louisiana State University
Baton Rouge, LA 70802
aganguly@lsu.edu

Abstract

Many systems in physics, engineering, and biology exhibit multiscale stochastic dynamics, where low-dimensional slow variables evolve under the influence of high-dimensional fast processes. In practice, observations are often limited to a single trajectory of the slow component, while the fast dynamics remain unobserved, making statistical learning challenging. Approaches based on partial differential equations (PDE), such as Fokker–Planck formulations, aim to characterize the evolution of probability densities, typically requiring dense space–time data or grid-based solvers. In contrast, we adopt a trajectory-based perspective and develop a data-driven framework for learning effective stochastic dynamics from a single observed path. We model the dynamics by coupled multiscale stochastic differential equations (SDEs) and first obtain a principled model reduction through stochastic averaging. Unlike generic model reduction techniques like PCA, this respects the dynamical structure of the original system and explicitly incorporates the interaction between slow and fast scales. A central challenge, however, is that the reduced model depends on the invariant distribution of the fast process which is a solution to an intractable and often unknown PDE. We introduce a novel learning framework that parameterizes the invariant distribution using normalizing flows, enabling expressive density modeling in the latent fast-variable space. The flow is trained end-to-end by optimizing a penalized likelihood objective induced by the reduced stochastic dynamics. Furthermore, we develop a Bayesian variational inference procedure for uncertainty quantification, employing a second normalizing flow to approximate the posterior distribution over model parameters. This yields a scalable approach to capturing epistemic uncertainty in multiscale systems. Our method bridges stochastic model reduction and flow-based latent density modeling, offering a scalable approach to learning effective dynamics in partially observed multiscale stochastic dynamical systems.

1 Introduction

Multiscale behavior is a defining feature of many stochastic systems arising in physics, engineering, and biology, where a few slow variables interact with rapidly evolving high-dimensional components [20]. Typical examples include molecular systems on complex energy landscapes, stochastic reaction networks with widely separated reaction rates, and climate systems coupling large-scale atmospheric evolution with rapidly fluctuating turbulence. In practice, one often has access only to a single observed trajectory of the slow variables, while the fast variables remain unobserved.

^{*}This research was supported in part by NSF grant DMS-2246815 and by the Simons Foundation through the Travel Support for Mathematicians program.

[†]Corresponding author.

Mathematically, such systems can be described through PDE formulations, such as Fokker–Planck or Kolmogorov equations, which govern the evolution of probability densities on the full state space [9, 21, 24]. These formulations are theoretically complete and useful in settings where either access to evolving densities or fine discretizations over the state space is available. However, their numerical implementation can become intractable in high-dimensional settings due to the cost solving PDEs. Furthermore, these approaches are not well-suited to data, consisting of a single observed trajectory.

A complementary viewpoint is provided by multiscale stochastic differential equations (SDEs) with scale separation. In this regime, a principle model-reduction can be achieved through stochastic averaging. This leads to a reduced-order SDE for the slow variables alone driven by averaged drift and diffusion functions where the effect of the fast variables are averaged out with respect to its invariant distribution. This reduction eliminates explicit dependence on fast variables while retaining the underlying dynamical structure.

The resulting reduced model, however, depends critically on the invariant distribution of the fast dynamics, which is typically unknown and only characterized implicitly through a high-dimensional stationary PDE. Consequently, even when the full multiscale system is specified, the effective coefficients governing the slow dynamics are not directly computable. This gives rise to a fundamental inference problem: learning the averaged driving functions, and hence the effective SDE dynamics, from partial trajectory observations in the presence of latent fast-scale equilibrium effects.

A natural statistical formulation of this problem is through maximum likelihood estimation (MLE), where the reduced SDE likelihood is optimized over all admissible probability measures on the state space of the fast variables (subject to suitable moment conditions). However, this infinite-dimensional optimization problem is computationally intractable and must be replaced by a tractable surrogate one that admits efficient parameterization and enables efficient optimization.

Contributions: The main contributions of this work are:

- We formulate inference for multiscale SDEs as a latent-invariant measure learning problem, where the effective drift and diffusion are expressed as conditional expectations with respect to an unknown invariant distribution of the fast process.
- We introduce a normalizing-flow parameterization of the latent invariant measure, which facilitates accurate approximation of the averaged functions governing the reduced dynamics.
- We develop a Bayesian extension using a second normalizing flow to approximate the posterior distribution over flow parameters, enabling uncertainty quantification for the inferred effective dynamics.
- We show that, under suitable conditions, the proposed flow-based estimators converge to MLE as the complexity of the underlying neural network (NN) increases.
- We validate the proposed method on synthetic multiscale systems, demonstrating accurate recovery of effective drift, matching of the true and estimated slow trajectories, as well as meaningful uncertainty estimates.

Overall, our approach bridges stochastic model reduction and flow-based probabilistic inference, providing a scalable framework for learning effective dynamics in partially observed multiscale stochastic systems.

2 Multiscale systems: Problem Setup

We consider multiscale stochastic system, where an observed slow component $X^{(n)}$ is coupled with a rapidly evolving latent process $Y^{(n)}$. The slow process $X^{(n)}$ satisfies the Itô SDE

$$dX^{(n)}(t) = b(X^{(n)}(t), Y^{(n)}(t)) dt + \sigma(X^{(n)}(t), Y^{(n)}(t)) dW(t), \quad (1)$$

where W is an \mathbb{R}^d -valued Brownian motion. The latent process $Y^{(n)}$ evolves on the fast time scale $O(1/n)$. We assume that the state spaces of $X^{(n)}$ and $Y^{(n)}$ are \mathbb{R}^d and $\mathbb{R}^{d'}$, respectively. $b : \mathbb{R}^d \times \mathbb{R}^{d'} \rightarrow \mathbb{R}^d$, $\sigma : \mathbb{R}^d \times \mathbb{R}^{d'} \rightarrow \mathbb{R}^{d \times d}$ denote the drift and diffusion coefficients and the parameter n captures the differences in speeds of the components.

To formalize the multiscale structure, we assume that $Y^{(n)}$ and the joint process $(X^{(n)}, Y^{(n)})$ are Markov with infinitesimal generator \mathcal{A}_n of $(X^{(n)}, Y^{(n)})$ given by

$$\mathcal{A}_n f(x, y) = \mathcal{A}_y^0 f(\cdot, y)(x) + n\mathcal{A}^1 f(x, \cdot)(y),$$

where

$$\mathcal{A}_y^0 \phi(x) = b(x, y) \cdot \nabla_x \phi(x) + \text{trace}(\sigma \sigma^\top(x, y) \nabla_x^2 \phi(x)).$$

Here \mathcal{A}_y^0 describes the evolution of the slow variable when the fast component is at state y , whereas $n\mathcal{A}^1$ is the generator of $Y^{(n)}$. If $Y^{(n)}$ is another Itô SDE of the form

$$dY^{(n)}(t) = n\beta(Y^{(n)}(t)) dt + \sqrt{n}\alpha(Y^{(n)}(t)) d\tilde{W}(t), \quad (2)$$

then \mathcal{A}^1 is given by

$$\mathcal{A}^1 \psi(y) = \beta(y) \cdot \nabla_y \psi(y) + \text{trace}(\alpha \alpha^\top(y) \nabla_y^2 \psi(y)). \quad (3)$$

If $Y^{(n)}$ is a continuous time Markov chain (CTMC) with state space $\mathbb{R}^{d'}$ then \mathcal{A}^1 has the form

$$\mathcal{A}^1 \psi(y) = c(y) \int (\psi(y') - \psi(y)) \nu(y, dy'), \quad (4)$$

where c is the jump intensity and ν is the (post-jump) transition probability kernel.

Goal: We consider the scenario when the fast Y -dynamics is unknown or intractable and the goal is to infer the effective dynamics of the system from observations of the slow X -component only. Specifically, we want to find a data-driven effective drift function $b_{\text{eff}} : \mathbb{R}^d \rightarrow \mathbb{R}^d$ and the diffusion function $\sigma_{\text{eff}} : \mathbb{R}^d \rightarrow \mathbb{R}^{d \times d}$, such that the SDE X_{eff} driven by them,

$$dX_{\text{eff}}(t) = b_{\text{eff}}(X_{\text{eff}}(t))dt + \sigma_{\text{eff}}(X_{\text{eff}}(t))dW(t)$$

mimics the dynamics of $X^{(n)}$.

This learning problem is intrinsically challenging because the fast Y -component is unobserved and typically has unknown dynamics. If the fast dynamics are known or can be reliably modeled, a naive inference strategy would attempt to reconstruct the latent trajectory of $Y^{(n)}$ jointly with the slow process. But this strategy is impractical and computationally expensive as $Y^{(n)}$ moves rapidly with much shortertime scale $O(1/n)$. For instance, if $Y^{(n)}$ is a fast continuous-time Markov chain with generator $n\mathcal{A}^1$ as in (4), then over any fixed time horizon $[0, T]$ one must precisely track $O(n)$ jump events. As a result, classical inference methods for stochastic differential equations (e.g., [28, 14, 8, 23, 2, 11, 13, 6, 3, 7, 16, 5, 26, 4]) are not directly applicable in this partially observed multiscale setting.

A naive inference strategy would attempt to reconstruct the latent trajectory of $Y^{(n)}$ jointly with the slow process. This is infeasible as the dynamics of $Y^{(n)}$ is typically not known. But even when it is known, the strategy is impractical and computationally expensive as $Y^{(n)}$ moves rapidly with time scale $O(1/n)$. For instance, if $Y^{(n)}$ is a fast continuous-time Markov chain with generator $n\mathcal{A}^1$, then that means over any fixed time horizon $[0, T]$ one needs to precisely track $O(n)$ jumps.

3 Methodology

Model Reduction through Stochastic averaging: Our first step is to obtain a model reduction of the given stochastic system. Standard techniques such as PCA and its variants are not suitable in this setting, as they do not respect the underlying dynamics. Instead, the reduction must be carried out in a principled manner that preserves the evolution of the slow X -component. This can be achieved via the stochastic averaging principle, and the following result, whose proof is given in the appendix, serves as the starting point for our inference problem.

Assumption 3.1. *There exists $V \in C^2(\mathbb{R}^d, [1, \infty))$ (called a Lyapunov function) such that the following hold:*

$$(i) \ c_* \stackrel{\text{def}}{=} -\limsup_{\|y\| \rightarrow \infty} \mathcal{A}^1 V(y) > 0$$

$$(ii) \ \nabla^\top V(y)(\alpha \alpha^\top(y)) \nabla V(y) = o(V(y)|\mathcal{A}^1 V(y)|) \text{ as } \|y\| \rightarrow \infty, \text{ that is,}$$

$$\frac{\nabla^\top V(y)(\alpha \alpha^\top(y)) \nabla V(y)}{V(y)|\mathcal{A}^1 V(y)|} \xrightarrow{\|y\| \rightarrow \infty} 0;$$

(iii) for some constant C_0 , exponents $p_0 \geq 0, 0 \leq \alpha_b, \alpha_\sigma \leq 1$,

$$\max \{ \|b(x, y) - b(x, y')\|, \|\sigma(x, y) - \sigma(x, y')\| \} \leq C_0 V(y)^{p_0} \|x - x'\|^{\alpha_0}.$$

(iv) (uniform ellipticity) for some constant $\lambda > 0$, $u^\top \alpha \alpha^\top(y) u \geq \lambda \|u\|^2$ for any $y, u \in \mathbb{R}^d$.

Theorem 3.2. Suppose that $Y^{(n)}$ satisfies the SDE (2) and Assumption 3.1 hold. Then, as $n \rightarrow \infty$, the slow process $X^{(n)} \xrightarrow{n \rightarrow \infty} X_{\pi_0}$, where

$$\begin{aligned} dX_{\pi_0}(t) &= \bar{b}_{\pi_0}(X_{\pi_0}(t)) dt + \bar{\sigma}_{\pi_0}(X_{\pi_0}(t)) dW(t), \\ \bar{b}_{\pi_0}(x) &= \int_{\mathbb{R}^{d'}} b(x, y) \pi_0(x, dy), \quad \bar{\sigma}_{\pi_0}(x) = \left(\int_{\mathbb{R}^{d'}} \sigma \sigma^\top(x, y) \pi_0 dy \right)^{1/2}, \end{aligned} \quad (5)$$

and π_0 is the unique stationary distribution of \mathcal{A}^1 in (3), i.e.,

$$(\mathcal{A}^1)^* \pi_0 = 0 \iff \int_{\mathbb{R}^{d'}} \mathcal{A}_x^1 \psi(y) \pi_0(dy) = 0 \quad \text{for all test functions } \psi. \quad (6)$$

The above result is also true when $Y^{(n)}$ is a jump-Markov process having generator $n\mathcal{A}^1$ with \mathcal{A}^1 as in (4). This provides a mathematical justification for a reduced model in which the influence of the high-dimensional fast variables enters only through their equilibrium effect on the slow dynamics, leading to a significant reduction in complexity. In other words, the limiting process X_{π_0} is playing the role of X_{eff} mentioned earlier with $b_{\text{eff}} \equiv \bar{b}_{\pi_0}$ and $\sigma_{\text{eff}} = \bar{\sigma}_{\pi_0}$, and the original inference problem is reformulated as one of learning \bar{b}_{π_0} and $\bar{\sigma}_{\pi_0}$ from the available X -observations.

However the main difficulty now lies in the dependence of \bar{b}_{π_0} and $\bar{\sigma}_{\pi_0}$ on the stationary distribution π_0 . This probability measure is unknown when the fast dynamics are not specified, but even when they are, π_0 cannot be computed efficiently as it is characterized implicitly through an intractable high-dimensional PDE as in (6).

Existing works on multiscale systems [19, 18, 10, 1] considered settings where the reduced drift has a known parametric structure, for example, $\bar{b}_{\pi_0}(x) = \vartheta_0 \tilde{b}(x)$, where \tilde{b} is known and $\vartheta_0 \equiv \vartheta_{\pi_0}$ is a finite-dimensional parameter depending on π_0 (e.g. moments of π_0). In such cases, the inference task simply reduces to estimating the finite-dimensional parameter ϑ_0 by standard methods.

In contrast, we consider a substantially more challenging setting in which the structural form of the averaged drift \bar{b}_{π_0} is completely unknown. Our aim is therefore to learn the effective dynamics in a fully nonparametric fashion, combining model reduction ideas from stochastic averaging with modern statistical and machine learning methodology.

A note about the learning problem: Crucially, our inferential target is \bar{b}_{π_0} , not π_0 . In general, the mapping $\pi \in \mathcal{P}(\mathbb{R}^d) \mapsto \bar{b}_\pi(\cdot)$ is not injective. For example, if $b(x, y) = b_0(x)y$, then $\bar{b}_\pi(x) = b_0(x)m$ depends only on the mean m of π , so infinitely many distinct invariant measures produce the same effective drift. For the class of SDEs considered here, it is \bar{b}_{π_0} that determines the reduced dynamics, governs the macroscopic behavior of the system, and is directly linked to the observable data through X . It is therefore the primary statistical object of interest: unlike π_0 , it is typically identifiable at the level of the reduced model and practically estimable from X -data. Nevertheless, if $b(\cdot, \cdot)$ is a characteristic kernel so that the map $\pi \mapsto \bar{b}_\pi(\cdot)$ becomes injective, then our method also recovers true π_0 .

3.1 Inference Setup

For simplicity, we assume in this paper that the diffusion function σ is known and does not depend on Y -component, i.e., $\sigma(x, y) = \sigma(x)$. Thus the inferential object is only $\bar{b}_{\pi_0}(\cdot) = \int b(\cdot, y) \pi_0(dy)$. We assume the kernel $b(\cdot, \cdot)$ is specified, so all uncertainty in the effective drift $\bar{b}_{\pi_0}(x) = \int b(x, y) \pi_0(dy)$ arises from the latent distribution π_0 , rather than from the local interaction structure $b(x, y)$ itself. This estimation task is particularly challenging because the unknown probability measure π_0 is an infinite-dimensional $\mathcal{P}(\mathbb{R}^{d'})$ -valued parameter, which cannot be estimated by conventional techniques.

Data and inference task: Our data consists of a high-frequency observation vector $\mathbf{x}_{0:M_0} \stackrel{\text{def}}{=} (x_0, x_1, \dots, x_{M_0})$ which is a realization of $(\bar{X}_{\pi_0})_{t_0:t_{M_0}} \stackrel{\text{def}}{=} (\bar{X}_{\pi_0}(t_0), \bar{X}_{\pi_0}(t_1), \dots, \bar{X}_{\pi_0}(t_{M_0}))$ —

discrete observations from \bar{X}_{π_0} at time points $\{t_m : m = 0, 1, 2, \dots, M_0\}$ satisfying $\Delta = t_m - t_{m-1} \ll 1$. Our objective is to compute an estimator \hat{b}_{π_0} based on the data $\mathbf{x}_{0:M_0}$.

We assume that the unknown $\pi_0 \in \mathcal{P}_{\text{abs}}^{(p)}(\mathbb{R}^{d'})$ for some $p \geq 0$. By Euler-Maruyama approximation, the (random) likelihood functional $L_T : C(\mathcal{X}, \mathbb{R}^d) \rightarrow \mathbb{R}$ for estimating the drift function \bar{b}_{π_0} is given by

$$L_T(\beta \mid \mathbf{x}_{0:M_0}) = \prod_{m=0}^{M_0-1} \frac{1}{(2\Delta\pi)^{d/2} \det^{1/2}(A(x_m))} e^{-R(\mathbf{x}_{0:M_0})/2\Delta} \quad (7)$$

$$\propto \exp \left\{ \sum_{m=0}^{M_0-1} \beta^\top(x_m) A^{-1}(x_m) (x_{m+1} - x_m - \beta(x_m)\Delta) - \frac{\Delta}{2} \sum_{m=0}^{M_0-1} \beta^\top(x_m) A^{-1}(x_m) \beta(x_m) \Delta \right\},$$

where $R(\mathbf{x}_{0:M_0}) \stackrel{\text{def}}{=} (x_{m+1} - x_m - \beta(x_m)\Delta)^\top A^{-1}(x_m) (x_{m+1} - x_m - \beta(x_m)\Delta)$ and $A(x) = \sigma\sigma^\top(x)$. An ideal estimator of course belongs to the class of maximum likelihood estimators (MLEs) defined as

$$\mathcal{M}_{\text{mle}} = \left\{ \bar{b}_{\hat{\rho}_*}(\cdot) \equiv \int b(\cdot, y) \hat{\rho}_*(dy) : \hat{\rho}_* \in \mathcal{A} \right\}, \quad (8)$$

where

$$\hat{\rho}_* \in \mathcal{A} \stackrel{\text{def}}{=} \arg \min \left\{ -\ln L_T(\bar{b}_\rho \mid \mathbf{x}_{0:M_0}) : \rho \in \mathcal{P}_{\text{abs}}^{(p)}(\mathbb{R}^{d'}) \right\}. \quad (9)$$

Notice that \mathcal{A} and \mathcal{M}_{mle} might not be singleton, i.e., a MLE estimator of \bar{b}_{π_0} is not unique.

3.2 Estimation procedure

Clearly, the optimization problem above is computationally infeasible, unless the state space of Y -component is simple (e.g., finite) or $b(\cdot, \cdot)$ has a simple structure (e.g., $b(x, y)$ is separable in x and y in the sense $b(x, y) = b_0(x)g_0(y)$). We approximate $\mathcal{P}_{\text{abs}}^{(p)}(\mathbb{R}^{d'})$ by a flexible parametric family $\mathcal{P}_n(\mathbb{R}^{d'})$ via flow f_θ :

$$\mathcal{P}_n(\mathbb{R}^{d'}) = \left\{ q^{(n)} \in \mathcal{P}(\mathbb{R}^{d'}) : q^{(n)} \equiv q_{\theta_n}^{(n)} = (f_{\theta_n}^{(n)})_{\#} \nu_{\text{ref}}, \theta_n \in \Theta_n \subset \mathbb{R}^{d'} \right\},$$

where $\#$ denotes the push-forward, and $f_{\theta_n}^{(n)}$ is modeled as a neural network (NN) with increasing complexity (depth, width) captured by n . Clearly, $Z \sim \nu_{\text{ref}} \implies f_\theta(Z) \sim q_\theta(\cdot)$. Unlike parametric families such as Gaussian mixtures, *flows* represent complex probability laws via a transformation of a simple reference distribution [22, 17]. Mathematically, the justification of replacing $\mathcal{P}_{\text{abs}}^{(p)}(\mathbb{R}^{d'})$ comes from Lemma 3.3, which shows any probability distribution in $\mathcal{P}_{\text{abs}}^{(p)}(\mathbb{R}^{d'})$ can be approximated by $\mathcal{P}_n(\mathbb{R}^{d'})$ as the complexity of the underlying neural network increases.

Lemma 3.3 (Wasserstein convergence of neural pushforwards). *Assume that for some $p \geq 1$, $\nu_{\text{ref}} \in \mathcal{P}_{\text{abs}}^{(p)}(\mathbb{R}^{d'})$. Fix any $\pi_0 \in \mathcal{P}_{\text{abs}}^{(p)}(\mathbb{R}^{d'})$. Then there exists a sequence of neural networks $\{f_{\theta_n} : \theta_n\}$ with non-polynomial activation function such that the family $\mathcal{P}_n(\mathbb{R}^{d'})$ is dense in $\mathcal{P}_{\text{abs}}^{(p)}(\mathbb{R}^{d'})$ under the Wasserstein- p metric, \mathcal{W}_p ; specifically, for any $\pi \in \mathcal{P}_{\text{abs}}^{(p)}(\mathbb{R}^{d'})$*

$$\lim_{n \rightarrow \infty} \inf_{\theta_n \in \Theta_n} \mathcal{W}_p \left(q_{\theta_n}^{(n)}, \pi \right) = 0.$$

The proof of the lemma is based on the Universal Approximation Theorem (UAT) and is provided in the appendix for completeness. Under certain extra assumptions, approximation rates of order $O(n^{-1/d})$ in \mathcal{W}_p -metric can be obtained, where n denotes the number of network parameters [27]. Thus flows form a highly expressive class of probability distributions suitable for *likelihood-based* inference problem that can approximate non-Gaussian, multimodal, and heavy-tailed distributions while still admitting efficient gradients and scalable optimization (for suitable architectures).

Flow based estimator: We now define the flow based estimator of \bar{b}_{π_0} . The main idea is to restrict the admissible class of probability measures in (9) to the family of pushforward measures $\mathcal{P}_n(\mathbb{R}^{d'})$ but

to ensure stability of the optimizer we look at a regularized (or penalized) optimization problem. For a probability measure $\rho \in \mathcal{P}_{\text{abs}}^{(p)}(\mathbb{R}^{d'})$, denote its p -th moment by $\mathbf{m}_p(\rho) = \int |y|^p \rho(dy)$, and define the penalized loss function $\mathcal{L}_\lambda : \mathcal{P}_{\text{abs}}^{(p)}(\mathbb{R}^{d'}) \rightarrow \mathbb{R}$ as

$$\mathcal{L}_\lambda(\rho) = -\ln L_T(\bar{b}_\rho | \mathbf{x}_{0:M_0}) + \lambda \mathbf{m}_p(\rho)$$

Next let

$$\hat{\theta}_{n,\lambda} = \operatorname{argmin}_{\theta_n \in \Theta_n} \mathcal{L}_\lambda(q_{\theta_n}^{(n)}). \quad (10)$$

and define the flow-based estimator of \bar{b}_{π_0} as

$$\bar{b}_{\hat{\theta}_{n,\lambda}}(\cdot) \stackrel{\text{def}}{=} \bar{b}_{q_{\hat{\theta}_{n,\lambda}}^{(n)}}(\cdot) \equiv \int_{\mathbb{R}^{d'}} b(\cdot, y) q_{\hat{\theta}_{n,\lambda}}^{(n)}(dy) \equiv \int_{\mathbb{R}^p} b(\cdot, f_{\hat{\theta}_{n,\lambda}}(z)) \nu_{\text{ref}}(dz). \quad (11)$$

Theorem 3.4 (Penalized parametric minimizers approach the global MLE set). *Fix $p > 1$ and define the MLE-set \mathcal{M}_{mle} and \mathcal{A} by (8) and (9). Suppose the drift-kernel $b(\cdot, \cdot)$ satisfies the following Lipschitz condition: there exists a locally bounded function $C_b : \mathbb{R}^d \rightarrow \mathbb{R}^d$ and exponent $0 \leq q_0 < p - 1$ such that*

$$\|b(x, y) - b(x, y')\| \leq C_b(x)(1 + \|y\|^{q_0} + \|y'\|^{q_0})\|y - y'\|. \quad (12)$$

Then for every $1 \leq p' < p$,

$$\lim_{\lambda \rightarrow 0} \limsup_{n \rightarrow \infty} \mathcal{W}_{p'}(q_{\hat{\theta}_{n,\lambda}}^{(n)}, \mathcal{A}) = 0. \quad (13)$$

For any compact set $K \subset \mathbb{R}^d$, Then

$$\lim_{\lambda \rightarrow 0} \limsup_{n \rightarrow \infty} \left\| \bar{b}_{\hat{\theta}_{n,\lambda}} - \mathcal{M}_{\text{mle}} \right\|_K = 0. \quad (14)$$

Thus the estimators $\bar{b}_{\hat{\theta}_{n,\lambda}}$ converges to the the MLE set \mathcal{M}_{mle} as the complexity of the parametric class (e.g. complexity of the underlying NN) increases and the penalty parameter λ decreases.

Monte-Carlo Approximation: Now fix a NN architecture $\{f_\theta : \theta \in \Theta\}$. In practice, the loss function $\mathcal{L}_\lambda(q_\theta)$ (where $q_\theta = (f_\theta)_{\#} \nu_{\text{ref}}$) requires the evaluation of $\bar{b}_\theta(\cdot) \equiv \bar{b}_{q_\theta}(\cdot) = \int_{\mathbb{R}^{d'}} b(\cdot, y) q_\theta(dy)$, and the integral is typically unavailable in closed form. We therefore use a Monte Carlo (MC) approximation at the observed states, $\bar{b}_\theta^{\text{MC}}(x_m) = \frac{1}{L} \sum_{l=1}^L b(x_m, f_\theta(Z^{(l)}))$ where $Z^{(l)} \stackrel{i.i.d.}{\sim} \nu_{\text{ref}}$, $l = 1, 2, \dots, L$. Notice that by the law of large numbers, $\bar{b}_\theta^{\text{MC}}(x_m) \rightarrow \bar{b}_\theta(x_m)$ as $L \rightarrow \infty$. In fact, under mild regularity conditions, this convergence is uniform in θ (assuming Θ is compact). It can then be shown that the estimator $\hat{\theta}^{\text{MC}}$, computed as

$$\hat{\theta}^{\text{MC}} \stackrel{\text{def}}{=} \operatorname{argmin}_{\theta \in \Theta} \mathcal{L}_\lambda(\bar{b}_\theta^{\text{MC}}),$$

converges to $\hat{\theta}$ as L increases. Note that, in order to evaluate the log-likelihood $\ln L_T(\bar{b}_\theta^{\text{MC}} | \mathbf{x}_{0:M_0})$, the MC approximation $\bar{b}_\theta^{\text{MC}}$ is required to be evaluated only at the finitely many observed states $\mathbf{x}_{0:M_0-1}$. An important advantage of the flow-based parametrization of q_θ is that it enables the use of the *reparameterization trick* for gradient-based optimization. Since the samples $Z^{(l)}$ are drawn from a fixed reference distribution ν_{ref} that does not depend on the NN parameter θ , gradients of $\ln L_T(\bar{b}_\theta^{\text{MC}} | \mathbf{x}_{0:M_0})$ can be computed by differentiating through the Monte Carlo approximation of the drift.

In particular, when computing $\nabla_\theta \ln L_T$, differentiation with respect to θ can be pushed inside the Monte Carlo sums, and the resulting derivatives act only through the map f_θ . At the integrand level, this involves the chain rule $\partial_\theta b(x, f_\theta(x, Z)) = \partial_y b(x, y)|_{y=f_\theta(x, Z)} \partial_\theta f_\theta(x, Z)$. This approach bypasses the need for the score-function estimator, which would require gradients of the density ρ_θ and typically suffers from high variance. By contrast, our formulation allows for high-precision, low-variance gradient estimates via standard backpropagation through the flow map f_θ .

3.3 Variational Inference

While the flow-based optimization described above performs well in many settings, principled uncertainty quantification requires a Bayesian formulation. To this end, we place a prior distribution $p_{\text{prior}}(\theta)$ over the neural network parameters. Applying Bayes' rule yields the posterior distribution

$$p_{\text{post}}(\theta \mid \mathbf{x}_{0:M_0}) = L_T(\bar{b}_\theta^{\text{MC}} \mid \mathbf{x}_{0:M_0}) p_{\text{prior}}(\theta) / p_{\text{marginal}}(\mathbf{x}_{0:M_0}), \quad (15)$$

where the normalization constant $p_{\text{marginal}}(\mathbf{x}_{0:M_0}) = \int L_T(\bar{b}_\theta^{\text{MC}} \mid \mathbf{x}_{0:M_0}) p_{\text{prior}}(\theta) d\theta$ does not depend on θ . However, since the parameter θ typically lies in a high-dimensional space, standard MCMC methods become computationally expensive and often impractical for posterior approximation. We adopt a variational inference framework to obtain a scalable approximation of the posterior p_{post} using a parametric family $\mathcal{P}_1(\Theta)$ induced by a flow g_ϑ :

$$\mathcal{P}_1(\Theta) = \left\{ \rho \in \mathcal{P}(\Theta) : \rho \equiv \rho_\vartheta = (g_\vartheta)_\# \rho_{\text{ref}}, \vartheta \in \mathcal{V} \right\}, \quad (16)$$

where g_ϑ is modeled using a neural network. The objective is to determine the optimal parameter by minimizing the reverse KL-divergence between the true posterior and its variational approximation:

$$\vartheta^* = \arg \min_{\vartheta \in \mathcal{V}} \text{KL}(\rho_\vartheta(\cdot) \parallel p_{\text{post}}(\cdot \mid \mathbf{x}_{0:M_0})).$$

Since the marginal likelihood does not depend on variational parameter ϑ , easy algebra shows that the above minimization problem is equivalent to maximizing the Evidence Lower Bound (ELBO):

$$\text{ELBO}(\vartheta) = \int_{\Theta} \ln L_T(\bar{b}_\theta^{\text{MC}} \mid \mathbf{x}_{0:M_0}) \rho_\vartheta(\theta) d\theta - \text{KL}(\rho_\vartheta \parallel p_{\text{prior}}). \quad (17)$$

Thus, the optimal parameter is obtained by

$$\vartheta^* = \arg \max_{\vartheta \in \mathcal{V}} \text{ELBO}(\vartheta).$$

To optimize the ELBO, we employ the reparameterization trick. Since $\rho_\vartheta = (g_\vartheta)_\# \rho_{\text{ref}}$, sampling from ρ_ϑ can be achieved by first drawing $\xi \sim \rho_{\text{ref}}$ and setting $\theta = g_\vartheta(\xi)$. This allows us to approximate the ELBO using Monte-Carlo samples:

$$\text{ELBO}(\vartheta) \approx \frac{1}{K} \sum_{k=1}^K \ln L_T(\bar{b}_{\theta^{(k)}}^{\text{MC}} \mid \mathbf{x}_{0:M_0}) - \text{KL}(\rho_\vartheta \parallel p_{\text{prior}}), \quad \theta^{(k)} = g_\vartheta(\xi^{(k)}), \xi^{(k)} \stackrel{\text{iid}}{\sim} \rho_{\text{ref}}.$$

This formulation enables efficient gradient-based optimization of the ELBO with respect to ϑ .

Algorithm 1 Flow-based Variational Inference for Integral-Drift SDEs

Require: Data $\mathbf{x}_{0:M_0}$, kernel $b(x, y)$, flows f_θ, g_ϑ , prior p_{prior} , sample sizes L, K

Ensure: Variational parameter $\hat{\vartheta}$

- 1: Initialize ϑ
 - 2: **repeat**
 - 3: Sample $\xi^{(1)}, \dots, \xi^{(K)} \sim \rho_{\text{ref}}$ (Reparameterization)
 - 4: Compute $\theta^{(k)} = g_\vartheta(\xi^{(k)})$, $k = 1, \dots, K$
 - 5: **for** $k = 1, \dots, K$ **do**
 - 6: Sample $Z^{(1)}, \dots, Z^{(L)} \sim \nu_{\text{ref}}$
 - 7: **for** $m = 0, \dots, M_0 - 1$ **do**
 - 8: Compute Monte-Carlo drift: $\bar{b}_{\theta^{(k)}}^{\text{MC}, L}(x_m) = \frac{1}{L} \sum_{l=1}^L b(x_m, f_{\theta^{(k)}}(Z^{(l)}))$
 - 9: **end for**
 - 10: **end for**
 - 11: Estimate Monte-Carlo ELBO
 - 12: Update ϑ using gradient ascent: $\vartheta \leftarrow \vartheta + \eta \nabla_{\vartheta} \text{ELBO}(\vartheta)$
 - 13: **until** convergence
 - 14: **return** $\hat{\vartheta}$
-

4 Experiments

Model: We consider a tagged particle interacting with a collection of solvent particles. The solvent configuration consists of N particles with positions $y_1, \dots, y_N \in \mathbb{R}^d$, whose interactions are governed by the quadratic potential

$$U_N(y_1, \dots, y_N) = \frac{a}{2} \sum_{i < j} \|y_i - y_j\|^2 + \frac{\kappa}{2} \sum_{i=1}^N \|y_i\|^2, \quad a, \kappa > 0. \quad (18)$$

This induces the following fast gradient type SDE (2) for $Y^{(n)}$ with drift $\beta(y) = -\gamma \nabla_y U_N(y)$, $\gamma > 0$, and $\alpha(y) = \sqrt{2}$. The corresponding invariant distribution is the Gibbs measure

$$\pi_0(dy_1, \dots, dy_N) \propto \exp(-\gamma U_N(y_1, \dots, y_N)) dy_1 \cdots dy_N. \quad (19)$$

The tagged particle $X^{(n)}$ interacts with the solvent through a pairwise potential V , yielding the drift

$$b(x, y_1, \dots, y_N) = - \sum_{i=1}^N \nabla_x V(\|x - y_i\|).$$

Under scale separation, the solvent rapidly equilibrates, and X_{π_0} satisfies SDE (6) with \bar{b}_{π_0} .

Experimental Design: Synthetic data are generated by simulating the multiscale SDE system given by (1) and (2) with the above drift and diffusion functions. This ground truth π_0 is only used for evaluating estimation accuracy. The SDE system is simulated over a fixed time horizon $[0, 5]$ using a fine discretization to obtain high-frequency observations. Importantly, evaluation of true averaged SDE with the estimated one is done beyond the observed time-interval

Computational Resources: Experiments were performed on an HPC node with dual Intel Xeon Gold 6342 CPUs and an NVIDIA A2 16 GB GPU using PyTorch.

Comparison: We compare the proposed structured estimator with a direct (unstructured) NN model for \bar{b}_{π_0} that ignores the integral representation $\bar{b}_{\pi_0}(x) = \int b(x, y) \pi_0(dy)$. This NN is trained by maximizing the likelihood induced by the Euler–Maruyama discretization of the corresponding SDE.

d	1	1	1	2	2
N	10	15	20	10	15
$n = 100$	0.02	0.0008	0.0053	0.0058	0.025
$n = 1000$	0.0029	0.0007	0.0004	0.0027	0.0035
$n = 15000$	0.0002	0.0002	0.0001	0.004	0.0055

Table 1: Mean squared errors for different datasets

Results: Table 4 reports the mean squared error (MSE) between the estimated and true averaged drift functions, evaluated on a grid of state values, and demonstrates the accuracy of the proposed method. In addition, we provide visual comparisons of the estimated and true drift functions, and plot trajectories of the true slow process alongside those generated by the SDE driven by the learned averaged drift (with a fixed random seed), both within and beyond the observation time window. The close agreement between these trajectories, even outside the observation window, is particularly noteworthy, as it demonstrates the predictive capability of the learned model beyond the range of observed data. This further indicates that the accuracy of the estimated averaged drift $\hat{\bar{b}}_{\pi_0}$ arises from genuine learning by the proposed method rather than overfitting. In contrast, the unstructured neural network model performs noticeably worse; for the first setting ($d = 1, N = 10$), it achieves MSE values of 0.014 and 0.008 for $n = 1000$ and $n = 15000$, respectively, which are approximately 10 times larger than those of the structured flow-based estimator.

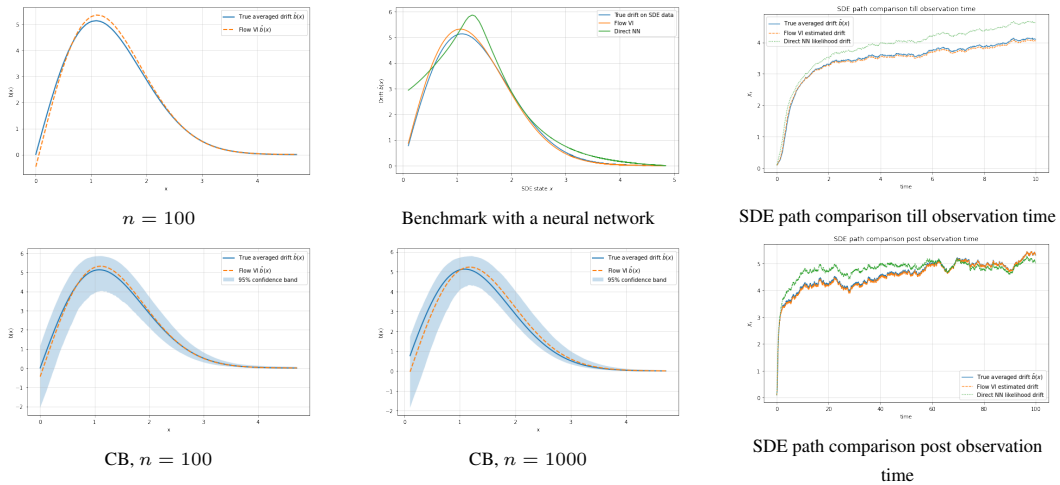


Figure 1: One-dimensional drift recovery with confidence bands.

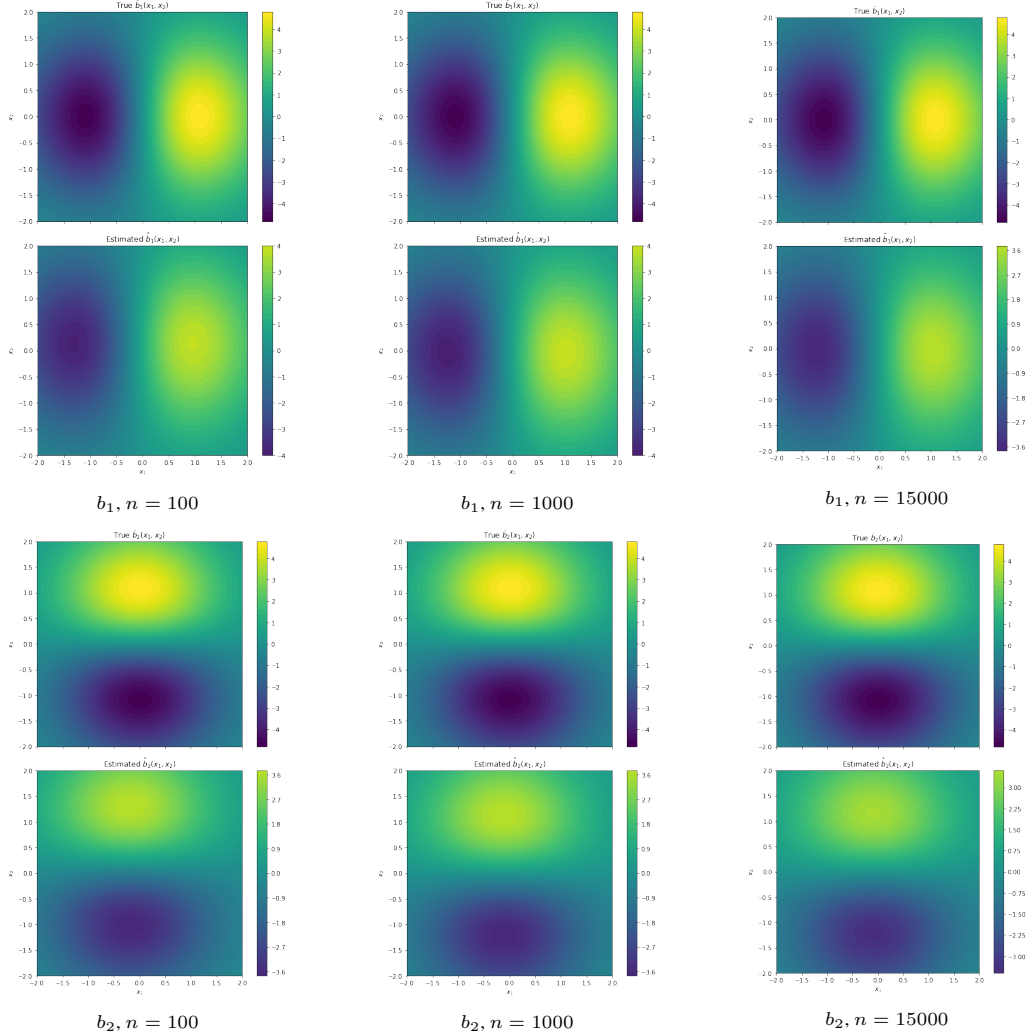


Figure 2: Two-dimensional drift recovery for the two drift components. The first row shows recovery of b_1 , and the second row shows recovery of b_2 , for increasing values of the scale parameter n .

5 Conclusion

We proposed a data-driven framework for learning effective dynamics in partially observed multiscale stochastic systems. A principled stochastic averaging reduction yields a lower-dimensional averaged SDE for the slow variables, where the drift depends on the invariant distribution of the latent fast process. We formulate inference as a latent-measure learning problem, parameterize this invariant measure using a normalizing flow, and train the resulting model via a likelihood objective based on reduced model. We show that penalized minimizers over increasingly expressive neural pushforward classes approach the global MLE under suitable assumptions. We further introduce a flow-based variational posterior to quantify uncertainty in the learned effective dynamics.

The performance of the method critically depends on the expressivity of the normalizing flow. The proposed approach, as described, does not directly apply to strongly coupled multiscale systems where the fast dynamics depend on the slow variables, nor to settings with sparse and noisy observations of the slow component. Extending the method to these regimes, together with the development of more expressive architectures based on continuous-time flows such as neural ODEs, constitutes an important direction for future work.

References

- [1] Assyr Abdulle, Giacomo Garegnani, Grigorios A Pavliotis, Andrew M Stuart, and Andrea Zanoni. Drift estimation of multiscale diffusions based on filtered data. *Foundations of Computational Mathematics*, 23(1):33–84, 2023.
- [2] Yacine Aït-Sahalia. Closed-form likelihood expansions for multivariate diffusions. *Ann. Statist.*, 36(2):906–937, 2008.
- [3] Cédric Archambeau and Manfred Opper. Approximate inference for continuous-time Markov processes. In *Bayesian time series models*, pages 125–140. Cambridge Univ. Press, Cambridge, 2011.
- [4] Jaya P. N. Bishwal. *Parameter estimation in stochastic volatility models*. Springer, Cham, 2022.
- [5] Mogens Bladt and Michael Sørensen. Simple simulation of diffusion bridges with application to likelihood inference for diffusions. *Bernoulli*, 20(2):645–675, 2014.
- [6] Jinyuan Chang and Song Xi Chen. On the approximate maximum likelihood estimation for diffusion processes. *Ann. Statist.*, 39(6):2820–2851, 2011.
- [7] Botond Cseke, Manfred Opper, and Guido Sanguinetti. Approximate inference in latent gaussian-markov models from continuous time observations. In C. J. C. Burges, L. Bottou, M. Welling, Z. Ghahramani, and K. Q. Weinberger, editors, *Advances in Neural Information Processing Systems 26*, pages 971–979. Curran Associates, Inc., 2013.
- [8] Ola Elerian, Siddhartha Chib, and Neil Shephard. Likelihood inference for discretely observed nonlinear diffusions. *Econometrica*, 69(4):959–993, 2001.
- [9] Yves Frederix, Giovanni Samaey, and Dirk Roose. An analysis of noise propagation in the multiscale simulation of coarse fokker-planck equations. *ESAIM: Mathematical Modelling and Numerical Analysis*, 45(3):541–561, 2011.
- [10] Siragan Gailus and Konstantinos Spiliopoulos. Discrete-time statistical inference for multiscale diffusions. *Multiscale Modeling & Simulation*, 16(4):1824–1858, 2018.
- [11] A. Golightly and D. J. Wilkinson. Bayesian inference for nonlinear multivariate diffusion models observed with error. *Comput. Statist. Data Anal.*, 52(3):1674–1693, 2008.
- [12] Kurt Hornik. Approximation capabilities of multilayer feedforward networks. *Neural networks*, 4(2):251–257, 1991.
- [13] Stefano M. Iacus. *Simulation and inference for stochastic differential equations*. Springer Series in Statistics. Springer, New York, 2008. With R examples.
- [14] Mathieu Kessler. Estimation of an ergodic diffusion from discrete observations. *Scand. J. Statist.*, 24(2):211–229, 1997.
- [15] Patrick Kidger and Terry Lyons. Universal approximation with deep narrow networks. In *Conference on learning theory*, pages 2306–2327. PMLR, 2020.
- [16] Chenxu Li. Maximum-likelihood estimation for diffusion processes via closed-form density expansions. *Ann. Statist.*, 41(3):1350–1380, 2013.
- [17] George Papamakarios, Eric Nalisnick, Danilo Jimenez Rezende, Shakir Mohamed, and Balaji Lakshminarayanan. Normalizing flows for probabilistic modeling and inference. *Journal of Machine Learning Research*, 22(57):1–64, 2021.
- [18] Grigorios A Pavliotis, Yvo Pokern, and Andrew M Stuart. Parameter estimation for multiscale diffusions: an overview. *Statistical methods for stochastic differential equations*, 124:429, 2012.
- [19] Grigorios A Pavliotis and AM Stuart. Parameter estimation for multiscale diffusions. *Journal of Statistical Physics*, 127(4):741–781, 2007.
- [20] Grigorios A. Pavliotis and Andrew M. Stuart. *Multiscale methods*, volume 53 of *Texts in Applied Mathematics*. Springer, New York, 2008. Averaging and homogenization.

- [21] Lukas Pichler, Arif Masud, and Lawrence A Bergman. Numerical solution of the fokker–planck equation by finite difference and finite element methods—a comparative study. In *Computational Methods in Stochastic Dynamics: Volume 2*, pages 69–85. Springer, 2013.
- [22] Danilo Rezende and Shakir Mohamed. Variational inference with normalizing flows. In *International conference on machine learning*, pages 1530–1538. PMLR, 2015.
- [23] G. O. Roberts and O. Stramer. On inference for partially observed nonlinear diffusion models using the Metropolis-Hastings algorithm. *Biometrika*, 88(3):603–621, 2001.
- [24] Timo Sprekeler, Endre Süli, and Zhiwen Zhang. Finite element approximation of stationary fokker–planck–kolmogorov equations with application to periodic numerical homogenization. *SIAM Journal on Numerical Analysis*, 63(3):1315–1343, 2025.
- [25] Cédric Villani et al. *Optimal transport: old and new*, volume 338. Springer, 2009.
- [26] Gavin A. Whitaker, Andrew Golightly, Richard J. Boys, and Chris Sherlock. Bayesian inference for diffusion-driven mixed-effects models. *Bayesian Anal.*, 12(2):435–463, 2017.
- [27] Yunfei Yang, Zhen Li, and Yang Wang. On the capacity of deep generative networks for approximating distributions. *Neural networks*, 145:144–154, 2022.
- [28] Nakahiro Yoshida. Estimation for diffusion processes from discrete observation. *J. Multivariate Anal.*, 41(2):220–242, 1992.

A Theoretical details and results

A.1 Stochastic averaging of fast-slow sde system

Proof of Theorem 3.2. Notice that $Y^{(n)}(\cdot) \stackrel{\text{Law}}{=} Y(n \cdot)$ where Y satisfies the SDE:

$$dY(t) = \beta(Y(t)) dt + \alpha(Y(t)) d\tilde{W}(t). \quad (20)$$

Fix $p > 1$. By Itô’s lemma

$$\begin{aligned} V^p(Y(t)) &= V^p(y_0) + p \int_0^t V^{p-1}(Y(s)) \mathcal{A}^1(Y(s)) ds \\ &\quad + p(p-1) \int_0^t V^{p-2}(Y(s)) \nabla^\top V(Y(s)) (\alpha \alpha^\top(Y(s))) \nabla V(Y(s)) ds + M_p(t), \end{aligned}$$

where $M_p(t) \stackrel{\text{def}}{=} p \int_0^t V^p(Y(s)) \nabla^\top V(Y(s)) \alpha(Y(s)) d\tilde{W}(s)$ is a martingale. Now by Assumption 3.1, for any $K > 0$, there exists an $R_K > 0$ such that for $\|y\| > R_0$,

$$\mathcal{A}^1 V(y) \leq -c_*/2, \quad \nabla^\top V(y) (\alpha \alpha^\top(y)) \nabla V(y) \leq \frac{1}{K} V(y) |\mathcal{A}^1 V(y)| \equiv -\frac{1}{K} V(y) \mathcal{A}^1 V(y).$$

By splitting the second integral according as $\|Y(s)\| > R_K$ or not we get for some constant C_p

$$\begin{aligned} V^p(Y(t)) &\leq V^p(y_0) + C_p t + (p - p(p-1)/K) \int_0^t V^{p-1}(Y(s)) \mathcal{A}^1(Y(s)) \mathbf{1}_{\{\|Y(s)\| > R_K\}} ds \\ &\quad + M_p(t). \end{aligned}$$

Choosing $K = 2p$, and using Assumption 3.1 it follows that

$$\sup_t \frac{1}{t} \int_0^t \mathbb{E} V^p(Y(s)) \mathbf{1}_{\{\|Y(s)\| > R_K\}} ds < \infty.$$

It follows that for any $t > 0$

$$\sup_t \frac{1}{t} \int_0^t \mathbb{E} V^p(Y(s)) ds \equiv \sup_t \mathbb{E} \int_{\mathbb{R}^d} V^p(y) \Gamma_t(dy) < \infty, \quad (21)$$

where the occupation measure $\{\Gamma_t\}$ of Y is defined by $\Gamma_t(A) = \frac{1}{t} \int_0^t \mathbf{1}_{\{Y(s) \in A\}} ds$. It follows that $\{\Gamma_t\}$ is tight as $\mathcal{P}(\mathbb{R}^{d'})$ -valued random variables. If η is a limit point of $\{\Gamma_t\}$, then by the Krylov-Bogoliubov theorem η is a stationary distribution of Y . Assumption 3.1:(iv) implies that Y is irreducible and hence admits a unique stationary distribution π_0 . Therefore, we have $\eta = \pi_0$, and thus $\Gamma_t \xrightarrow{t \rightarrow \infty} \pi_0$ in probability in the space $\mathcal{P}(\mathbb{R}^{d'})$. Furthermore, since (21) holds, for any function f satisfying $f = O(V^p)$ for some $p > 0$, $\frac{1}{t} \int_0^t f(Y(s)) ds = \int f(y) \Gamma_t(dy) \xrightarrow{t \rightarrow \infty} \int f(y) \pi_0(dy)$.

Now by a simple change of variable formula we have for any (measurable) function f , $\int_0^t f(Y^{(n)}(s)) ds \stackrel{\text{Law}}{=} \frac{1}{n} \int_0^{nt} f(Y(s)) ds$. and thus for any fixed $T > 0$ Define the random measure $\Gamma^{(n)}$ on $\mathbb{R}^d \times [0, t]$ as $\Gamma^{(n)}(A \times [0, t]) = \int_{\mathbb{R}^d \times [0, t]} \mathbf{1}_{\{Y^{(n)}(s) \in A\}} ds$. It follows that $\Gamma^{(n)} \xrightarrow{n \rightarrow \infty} \pi_0 \otimes \text{Leb}$ and that for any continuous $g : \mathbb{R}^{d'} \times [0, T] \rightarrow \mathbb{R}^{d''}$ satisfying $\sup_{s \leq T} \|g(y, s)\| \leq C_g V^p(s)$ for some $p > 0$, we have

$$\int_{\mathbb{R}^d \times [0, t]} g(y, s) \Gamma^{(n)}(dy \times ds) \equiv \int_{\mathbb{R}^d \times [0, t]} g(Y^{(n)}(s), s) ds \xrightarrow{n \rightarrow \infty} \int_{\mathbb{R}^d \times [0, t]} f(y, s) \pi_0(dy) ds. \quad (22)$$

Next, simple estimates show that $\sup_{0 \leq t, t+h \leq T} \mathbb{E}(\|X^{(n)}(t+h) - X^{(n)}(t)\|^2) = O(h^\alpha)$ from which it follows that the sequence $\{X_n\}$ is tight in $C([0, T], \mathbb{R}^d)$. Let X is a limit point of $\{X_n\}$. By Skorohod representation theorem we can assume without loss of generality that $X_n \rightarrow X$ a.s. in $C([0, T], \mathbb{R}^d)$ along a subsequence, which for notational convenience we continue to index by n . We next show that

$$\int_0^t (b(X_n(s), Y_n(s)) ds \xrightarrow{n \rightarrow \infty} \int_{\mathbb{R}^{d'} \times [0, t]} (b(X(s), y) \pi_0(dy) ds = \bar{b}_{\pi_0}(X(s)). \quad (23)$$

To this end, write

$$\int_0^t (b(X_n(s), Y_n(s)) ds = \int_{\mathbb{R}^{d'} \times [0, t]} (b(X_n(s), y) \Gamma^n(dy \times ds) = I_1(t) + I_2(t),$$

where by Assumption 3.1, (22) as $n \rightarrow \infty$

$$\begin{aligned} \sup_{t \leq T} |I_1(t)| &= \sup_{t \leq T} \left| \int_0^t ((b(X_n(s), Y_n(s)) - b(X(s), Y_n(s))) ds \right| \\ &\leq C_0 \sup_{t \leq T} |X_n(t) - X(t)|^{\alpha_0} \int_0^T V^{p_0}(Y^{(n)}(s)) ds \xrightarrow{\mathbb{P}} 0. \end{aligned}$$

Next by (22)

$$\begin{aligned} I_2(t) &= \int_0^t b(X_n(s), Y_n(s)) ds \equiv \int_{\mathbb{R}^{d'} \times [0, t]} (b(X(s), y) \Gamma^n(dy \times ds) \\ &\xrightarrow{n \rightarrow \infty} \int_{\mathbb{R}^{d'} \times [0, t]} (b(X(s), y) \pi_0(dy) ds = \bar{b}_{\pi_0}(X(s)), \end{aligned}$$

which proves (24). Similarly, by Burkholder-Davis-Gundy inequality it follows that

$$E \left[\sup_{t \leq T} \left| \int_0^t ((\sigma(X_n(s), Y_n(s)) - \sigma(X(s), Y_n(s))) dW(s) \right|^2 \right] \xrightarrow{n \rightarrow \infty} 0.$$

Notice that for the martingale term $M^{(n)}(\cdot) = \int_0^\cdot \sigma(X(s), Y_n(s)) dW(s)$ has the quadratic variation given by

$$[M^{(n)}]_t = \int_0^t \sigma \sigma^\top(X(s), Y_n(s)) ds \xrightarrow{n \rightarrow \infty} \int_{\mathbb{R}^{d'} \times [0, t]} \sigma \sigma^\top(X(s), y) \pi_0(dy) ds \equiv \bar{\sigma}_{\pi_0}^2(X(s)).$$

It follows by the Martingale CLT that as $n \rightarrow \infty$

$$M^{(n)}(t) \stackrel{\text{Law}}{\rightarrow} \bar{\sigma}_{\pi_0}(X(s)). \quad (24)$$

Therefore the limit point X satisfies (5), and since this SDE admits a unique solution the result follows. \square

A.2 Wasserstein convergence of neural pushforwards

Proof of Lemma 3.3. Since $\nu_{\text{ref}}, \pi_0 \in \mathcal{P}_{\text{abs}}^{(p)}(\mathbb{R}^{d'})$, there exists a measurable transport map $T : \mathbb{R}^{d'} \rightarrow \mathbb{R}^{d'}$ such that

$$T_{\#}\nu_{\text{ref}} = \pi_0.$$

This follows, for instance, from the Knothe–Rosenblatt rearrangement or Brenier’s theorem under absolute continuity.

Next, we use the universal approximation theorem in $L^p(\mu)$ for general measures. By [12], finite neural networks with non-polynomial activation functions are dense in $L^p(\mu)$ for any finite measure μ (also see [15]). Taking $\mu = \nu_{\text{ref}}$, there exists a finite neural network with non-polynomial activation such that, $f : \mathbb{R}^{d'} \rightarrow \mathbb{R}^{d'}$ such that

$$\|f - T\|_{L^p(\nu_{\text{ref}})} = \left(\int_{\mathbb{R}^{d'}} \|f(x) - T(x)\|^p \nu_{\text{ref}}(dx) \right)^{1/p} < \varepsilon.$$

Define the coupling

$$\gamma := (T, f)_{\#}\nu_{\text{ref}}.$$

Then γ is a valid coupling between $T_{\#}\nu_{\text{ref}} = \pi_0$ and $f_{\#}\nu_{\text{ref}}$. Therefore, by definition of Wasserstein distance,

$$W_p^p(\pi_0, f_{\#}\nu_{\text{ref}}) \leq \int_{\mathbb{R}^{d'}} \|T(x) - f(x)\|^p \nu_{\text{ref}}(dx).$$

Taking the p th root yields

$$W_p(\pi_0, f_{\#}\nu_{\text{ref}}) \leq \|f - T\|_{L^p(\nu_{\text{ref}})} < \varepsilon.$$

This completes the proof. □

A.3 Penalized Likelihood Convergence

Lemma A.1. *Let $p > 1$ and $C > 0$. The set $\mathcal{P}_C^{(p)} \stackrel{\text{def}}{=} \left\{ \eta \in \mathcal{P}(\mathbb{R}^{d'}) : \mathfrak{m}_p(\eta) \equiv \int \|y\|^p \eta(dy) \leq C \right\}$ is compact in weak topology of $\mathcal{P}(\mathbb{R}^{d'})$. If $\tilde{\eta}$ is a limit point of $\mathcal{P}_C^{(p)}$ with $\mathcal{P}_C^{(p)} \ni \eta_n \xrightarrow{n \rightarrow \infty} \tilde{\eta}$, then $\mathcal{W}_{p'}(\eta_n, \tilde{\eta}) \xrightarrow{n \rightarrow \infty} 0$ for any $1 \leq p' < p$. In particular, $\mathcal{P}_C^{(p)}$ is also compact in $(\mathcal{P}(\mathbb{R}^{d'}), \mathcal{W}_{p'})$ for any $1 \leq p' < p$.*

Proof of Lemma A.1. This is a standard consequence of Prokhorov’s theorem together with bounded p -moment compactness in Wasserstein space; see [25, Theorem 6.9]. □

Proof of Theorem 3.4. The following observation is crucial to the proof. Suppose $\{\eta_n\} \subset \mathcal{P}_C^{(p)}$ and for some $p' \in [1, p]$

$$\mathcal{W}_{p'}(\eta_n, \tilde{\eta}) \xrightarrow{n \rightarrow \infty} 0. \tag{25}$$

- Notice that (12) implies that for each x , $b(x, \cdot)$ satisfies the following growth condition: $b(x, y) = O(\|y\|^{q_0+1})$. Hence, if $p' \geq q_0 + 1$, then for any $x \in \mathbb{R}^d$,

$$\bar{b}_{\eta_n}(x) \equiv \int b(x, y) \eta_n(dy) \xrightarrow{n \rightarrow \infty} \bar{b}_{\tilde{\eta}}(x) \equiv \int b(x, y) \tilde{\eta}(dy),$$

whence it follows that for $q_0 + 1 \leq p' < p$

$$\lim_{n \rightarrow \infty} \ln L_T(\bar{b}_{\eta_n} \mid \mathbf{x}_{0:M_0}) = \ln L_T(\bar{b}_{\tilde{\eta}} \mid \mathbf{x}_{0:M_0}), \quad \text{and} \quad \liminf_{n \rightarrow \infty} \mathcal{L}_{\lambda}(\eta_n) \geq \mathcal{L}_{\lambda}(\tilde{\eta}). \tag{26}$$

The second part of (26) uses lower semicontinuity of the map $\eta \rightarrow \mathfrak{m}_p(\eta)$. Now observe that if $\{\lambda_n\}$ is a sequence such that $\lambda_n \rightarrow 0$, then the first part of (26) and the fact that $\sup_n \mathfrak{m}_p(\eta_n) \leq C$ shows that

$$\lim_{n \rightarrow \infty} \mathcal{L}_{\lambda_n}(\eta_n) = -\ln L_T(\bar{b}_{\tilde{\eta}} \mid \mathbf{x}_{0:M_0}). \tag{27}$$

- If in fact $\mathcal{W}_p(\eta_n, \eta) \xrightarrow{n \rightarrow \infty} 0$ (i.e., $p' = p$), then $\mathfrak{m}_p(\eta_n) \rightarrow \mathfrak{m}_p(\eta)$, and hence

$$\lim_{n \rightarrow \infty} \mathcal{L}_\lambda(\eta_n) = \mathcal{L}_\lambda(\eta). \quad (28)$$

- Suppose the convergence in (25) holds for some $p/(p - q_0) \leq p' \leq p$. Then notice that $q_0 p'/(p' - 1) \leq p$, and hence

$$\sup_n \mathfrak{m}_{q_0 p'/(p'-1)}(\eta_n) \vee \mathfrak{m}_{q_0 p'/(p'-1)}(\eta) < \infty.$$

Now recalling that $C_b : \mathbb{R}^d \rightarrow [0, \infty)$ in (12) is locally bounded, we have from Lemma A.1 for any compact set $K \subset \mathbb{R}^d$

$$\begin{aligned} \|\bar{b}_{\eta_n} - \bar{b}_\eta\|_K &\equiv \sup_{x \in K} |\bar{b}_{\eta_n}(x) - \bar{b}_\eta(x)| \\ &\leq 3^{1/p'} \sup_{x \in K} C_b(x) \left(1 + \sup_n \mathfrak{m}_{q_0 p'/(p'-1)}(\eta_n) + \mathfrak{m}_{q_0 p'/(p'-1)}(\eta) \right)^{(p'-1)/p'} \mathcal{W}_{p'}(\eta_n, \eta) \xrightarrow{n \rightarrow \infty} 0. \end{aligned} \quad (29)$$

We next establish the following claim.

Claim: Fix any $\hat{\rho}_\lambda \in \mathcal{A}_\lambda \stackrel{def}{=} \arg \min_{\rho \in \mathcal{P}^{(p)}(\mathbb{R}^{d'})} \mathcal{L}_\lambda(\rho)$. Then for any $1 \leq p' < p$, $\lim_{\lambda \rightarrow 0} \mathcal{W}_{p'}(\hat{\rho}_\lambda, \mathcal{A}) = 0$. Furthermore, for any compact set $K \subset \mathbb{R}^d$, $\lim_{\lambda \rightarrow 0} \|\bar{b}_{\hat{\rho}_\lambda} - \mathcal{M}_{\text{mle}}\|_K = 0$.

It is easy to see that $\mathcal{A}_\lambda \neq \emptyset$. Now notice that by the definition of $\hat{\rho}_*$ (see (9)), $\hat{\rho}_\lambda$

$$-\ln L_T(\bar{b}_{\hat{\rho}_*} | \mathbf{x}_{0:M_0}) \leq -\ln L_T(\bar{b}_{\hat{\rho}_\lambda} | \mathbf{x}_{0:M_0}) \leq \mathcal{L}_\lambda(\hat{\rho}_\lambda) \leq \mathcal{L}_\lambda(\hat{\rho}_*) \equiv -\ln L_T(\bar{b}_{\hat{\rho}_*} | \mathbf{x}_{0:M_0}) + \lambda \mathfrak{m}_p(\hat{\rho}_*). \quad (30)$$

This implies

$$0 \leq \mathcal{L}_\lambda(\hat{\rho}_\lambda) + \ln L_T(\bar{b}_{\hat{\rho}_*} | \mathbf{x}_{0:M_0}) \equiv (\ln L_T(\bar{b}_{\hat{\rho}_*} | \mathbf{x}_{0:M_0}) - \ln L_T(\bar{b}_{\hat{\rho}_\lambda} | \mathbf{x}_{0:M_0})) + \lambda \mathfrak{m}_p(\hat{\rho}_\lambda) \leq \lambda \mathfrak{m}_p(\hat{\rho}_*).$$

Since $\ln L_T(\bar{b}_{\hat{\rho}_*} | \mathbf{x}_{0:M_0}) - \ln L_T(\bar{b}_{\hat{\rho}_\lambda} | \mathbf{x}_{0:M_0}) \geq 0$, it follows that $\lambda \mathfrak{m}_p(\hat{\rho}_\lambda) \leq \lambda \mathfrak{m}_p(\hat{\rho}_*)$, i.e., for any $\lambda > 0$, $\mathfrak{m}_p(\hat{\rho}_\lambda) \leq \mathfrak{m}_p(\hat{\rho}_*)$. By Lemma A.1, the family $\{\hat{\rho}_\lambda\}$ is relatively compact in weak topology of $\mathcal{P}(\mathbb{R}^{d'})$ and $(\mathcal{P}(\mathbb{R}^{d'}), \mathcal{W}_{p'})$ for any $p' < p$. If $\tilde{\rho}_*$ is one of its limit points and $\{\lambda_n\} \rightarrow 0$ is a subsequence such that $\hat{\rho}_{\lambda_n} \xrightarrow{k \rightarrow \infty} \tilde{\rho}_*$ then for any $p' < p$,

$$\lim_{k \rightarrow \infty} \mathcal{W}_{p'}(\hat{\rho}_{\lambda_n}, \tilde{\rho}_*) = 0 \quad (31)$$

Since, in particular, (31) holds for $q_0 + 1 \leq p' < p$, it follows by (27) that $\lim_{n \rightarrow \infty} \mathcal{L}_{\lambda_n}(\hat{\rho}_{\lambda_n}) = -\ln L_T(\bar{b}_{\tilde{\rho}_*} | \mathbf{x}_{0:M_0})$. Consequently, taking $\lambda_n \rightarrow 0$ we get from (30),

$$\ln L_T(\bar{b}_{\tilde{\rho}_*} | \mathbf{x}_{0:M_0}) = \ln L_T(\bar{b}_{\hat{\rho}_{\lambda_n}} | \mathbf{x}_{0:M_0}) \implies \tilde{\rho}_* \in \mathcal{A} \implies \lim_{n \rightarrow \infty} \mathcal{W}_{p'}(\hat{\rho}_{\lambda_n}, \mathcal{A}) = 0.$$

Thus $\tilde{\rho}_* \in \mathcal{M}_{\text{mle}}$, and since (31), in particular, holds for $p/(p - q_0) \leq p' < p$, we have by (29)

$$\|\bar{b}_{\hat{\rho}_{\lambda_n}} - \mathcal{M}_{\text{mle}}\|_K \leq \sup_{x \in K} |\bar{b}_{\hat{\rho}_{\lambda_n}}(x) - \bar{b}_{\tilde{\rho}_*}(x)| \xrightarrow{n \rightarrow \infty} 0.$$

As these limits hold independent of the choice of the specific subsequence $\{\lambda_n\}$, the claim follows.

We next show that $\{q_{\theta_{n,\lambda}}^{(n)}\}$ in Theorem 3.4 is relatively compact in $(\mathcal{P}(\mathbb{R}^{d'}), \mathcal{W}_{p'})$ for any $p' < p$.

To this end, first notice that $\ln L_T(\bar{b}_\rho | \mathbf{x}_{0:M_0}) \leq C_0(\mathbf{x}_{0:M_0})$, where the constant $C_0(\mathbf{x}_{0:M_0}) \equiv -\left(M_0 d \ln(2\Delta\pi)/2 + \frac{1}{2} \sum_{m=0}^{M_0-1} \ln(\det A(x_m))\right)$, does not depend on ρ . It follows that

$$\mathcal{L}_\lambda(\rho) \geq -C_0(\mathbf{x}_{0:M_0}) + \lambda \mathfrak{m}_p(\rho) \geq -C_0(\mathbf{x}_{0:M_0}), \quad (32)$$

and hence

$$\mathcal{L}_\lambda^* \stackrel{def}{=} \inf_{\rho \in \mathcal{P}^{(p)}(\mathbb{R}^{d'})} \mathcal{L}_\lambda(\rho) \in (-\infty, \infty).$$

Fix an $\varepsilon > 0$, and let $\rho_{\lambda,\varepsilon} \in \mathcal{P}^{(p)}(\mathbb{R}^{d'})$ be such that $\mathcal{L}_\lambda(\rho_{\lambda,\varepsilon}) \leq \mathcal{L}_\lambda^* + \varepsilon$. By Lemma 3.3, there exists a sequence $\{\hat{\theta}_{n,\lambda,\varepsilon}\}$ such that

$$\mathcal{W}_p\left(q_{\hat{\theta}_{n,\lambda,\varepsilon}}^{(n)}, \rho_{\lambda,\varepsilon}\right) \xrightarrow{n \rightarrow \infty} 0.$$

It follows from (28), (32) and by the definition of $\hat{\theta}_{n,\lambda}$ (see (10)) that there exists N_0 such that for all $n \geq N_0$

$$\begin{aligned} -C_0(\mathbf{x}_{0:M_0}) + \lambda \mathfrak{m}_p\left(q_{\hat{\theta}_{n,\lambda}}^{(n)}\right) &\leq \mathcal{L}_\lambda\left(q_{\hat{\theta}_{n,\lambda}}^{(n)}\right) \leq \mathcal{L}_\lambda\left(q_{\hat{\theta}_{n,\lambda,\varepsilon}}^{(n)}\right) \leq \mathcal{L}_\lambda^* + 2\varepsilon \\ \implies \mathfrak{m}_p\left(q_{\hat{\theta}_{n,\lambda}}^{(n)}\right) &\leq \lambda^{-1}(\mathcal{L}_\lambda^* + 2\varepsilon + C_0(\mathbf{x}_{0:M_0})). \end{aligned} \quad (33)$$

By Lemma A.1, the sequence $\{q_{\hat{\theta}_{n,\lambda}}^{(n)}\}$ is relatively compact in weak topology of $\mathcal{P}(\mathbb{R}^{d'})$ and $(\mathcal{P}(\mathbb{R}^{d'}), \mathcal{W}_{p'})$ for any $p' < p$. If $q_{\lambda,*}$ is one of its limit points and $\{q_{\hat{\theta}_{n_k,\lambda}}^{(n_k)}\}$ is a subsequence such that $q_{\hat{\theta}_{n_k,\lambda}}^{(n_k)} \xrightarrow{k \rightarrow \infty} q_{\lambda,*}$ then for any $p' < p$

$$\lim_{k \rightarrow \infty} \mathcal{W}_{p'}\left(q_{\hat{\theta}_{n_k,\lambda}}^{(n_k)}, q_{\lambda,*}\right) = 0. \quad (34)$$

In particular, (34) holds for $q_0 + 1 \leq p' < p$, and hence by (33), the second part of (26) and the definition of \mathcal{L}_λ^* that

$$\mathcal{L}_\lambda^* \leq \mathcal{L}_\lambda(q_{\lambda,*}) \leq \liminf_k \mathcal{L}_\lambda\left(q_{\hat{\theta}_{n_k,\lambda}}^{(n_k)}\right) \leq \mathcal{L}_\lambda^* + 2\varepsilon.$$

Since ε is arbitrary, it follows $\mathcal{L}_\lambda(q_{\lambda,*}) = \mathcal{L}_\lambda^*$, i.e., $q_{\lambda,*} \in \mathcal{A}_\lambda$. Next by using the fact that (34), in particular, holds for $p/(p - q_0) \leq p' < p$, we have by (29)

$$\left\| \bar{b}_{\hat{\theta}_{n_k,\lambda}} - \bar{b}_{q_{\lambda,*}} \right\|_K \equiv \sup_{x \in K} \left\| \bar{b}_{\hat{\theta}_{n_k,\lambda}}(x) - \bar{b}_{q_{\lambda,*}}(x) \right\| \xrightarrow{n \rightarrow \infty} 0, \quad (35)$$

where recall for notational simplicity, we denote $\bar{b}_{\hat{\theta}_{n,\lambda}} \stackrel{def}{=} \bar{b}_{q_{\hat{\theta}_{n,\lambda}}^{(n)}}$ (see (11)).

Now by the triangle inequality,

$$\begin{aligned} \mathcal{W}_{p'}\left(q_{\hat{\theta}_{n_k,\lambda}}^{(n)}, \mathcal{A}\right) &\leq \mathcal{W}_{p'}\left(q_{\hat{\theta}_{n_k,\lambda}}^{(n)}, q_{\lambda,*}\right) + \mathcal{W}_{p'}\left(q_{\lambda,*}, \mathcal{A}\right) \\ \left\| \bar{b}_{\hat{\theta}_{n_k,\lambda}} - \mathcal{M}_{\text{mle}} \right\|_K &\leq \left\| \bar{b}_{\hat{\theta}_{n_k,\lambda}} - \bar{b}_{q_{\lambda,*}} \right\|_K + \left\| \bar{b}_{q_{\lambda,*}} - \mathcal{M}_{\text{mle}} \right\|_K. \end{aligned}$$

It follows from (34), (35) and the *claim* that

$$\lim_{\lambda \rightarrow 0} \lim_{k \rightarrow \infty} \mathcal{W}_{p'}\left(q_{\hat{\theta}_{n_k,\lambda}}^{(n)}, \mathcal{A}\right) = 0, \quad \lim_{\lambda \rightarrow 0} \lim_{k \rightarrow \infty} \left\| \bar{b}_{\hat{\theta}_{n_k,\lambda}} - \mathcal{M}_{\text{mle}} \right\|_K = 0.$$

Since these limits are independent of choice of the specific subsequence $\{n_k\}$, (13) and (14) hold. \square

B Neural network architecture

We use normalizing flows at two levels. The first flow, f_θ , parameterizes the latent invariant distribution $q_\theta = (f_\theta)_{\#} \nu_{\text{ref}}$ appearing in the integral drift. The second flow, g_ϑ , parameterizes the variational distribution $\rho_\vartheta = (g_\vartheta)_{\#} \rho_{\text{ref}}$ over the parameters θ of f_θ . Both maps are implemented using RealNVP affine coupling layers.

RealNVP architecture. Let $h_\phi : \mathbb{R}^m \rightarrow \mathbb{R}^m$ denote a generic RealNVP flow with parameter ϕ . The map is written as a composition of K_{flow} affine coupling layers,

$$y^0 = z, \quad y^k = h_\phi^{(k)}(y^{k-1}), \quad k = 1, \dots, K_{\text{flow}},$$

and $h_\phi(z) = y^{K_{\text{flow}}}$. At layer k , the input is split as

$$y^{k-1} = (y_a^{k-1}, y_b^{k-1}), \quad m_a + m_b = m.$$

The affine coupling transformation is

$$\begin{aligned} y_a^k &= y_a^{k-1}, \\ y_b^k &= y_b^{k-1} \odot \exp\left(s_\phi^{(k)}(y_a^{k-1})\right) + t_\phi^{(k)}(y_a^{k-1}), \end{aligned} \quad (36)$$

where

$$s_\phi^{(k)}, t_\phi^{(k)} : \mathbb{R}^{m_a} \rightarrow \mathbb{R}^{m_b}$$

are feed-forward neural networks, and \odot denotes componentwise multiplication. Alternating binary masks are used across layers so that all coordinates are transformed through the composition.

The triangular structure of (36) gives a tractable Jacobian determinant:

$$\log \left| \det \frac{\partial h_\phi(z)}{\partial z} \right| = \sum_{k=1}^{K_{\text{flow}}} \sum_{i=1}^{m_b} s_\phi^{(k)}(y_a^{k-1})_i. \quad (37)$$

Thus density evaluation and sampling are both efficient.

C Training details

All models are trained using the Adam optimizer with learning rate 10^{-3} . We do not use a learning-rate scheduler. To stabilize optimization, gradient norms are clipped at 5.0. Training is performed for 100 variational iterations. At each iteration, a minibatch of size $B = 500$ is sampled uniformly from the observed trajectory, and the minibatch log-likelihood is rescaled by M_0/B to approximate the full-data contribution to the ELBO.

The ELBO is estimated using nested Monte Carlo sampling. We use $K = 100$ samples from the variational distribution ρ_θ and $L = 100$ latent samples from ν_{ref} for each sampled parameter. To reduce memory usage, both Monte Carlo levels are evaluated in batches: the parameter samples are processed with batch size 20, and the latent samples are processed with batch size 25.

The latent transport map f_θ is implemented as a RealNVP flow with 2 affine coupling layers and hidden dimension 5. The variational posterior flow g_θ is implemented as a RealNVP flow with 6 affine coupling layers and hidden dimension 256. We use $N = 10$ latent particles, so that the latent dimension is

$$D = N \cdot d.$$

The kernel scale is fixed at $\zeta = 1.0$, the diffusion coefficient is fixed at $\sigma = 0.1$, and the Euler-Maruyama step size is $\Delta = 0.01$.

For posterior evaluation, we use 500 samples from the variational distribution and 1000 latent samples per parameter sample. These computations are also performed using batching, with parameter batch size 20 and latent batch size 100.

D Further experiments

Finite-time law comparison for non-ergodic dynamics: We compare the finite-time marginal laws of the true averaged SDE and the learned averaged SDE.

For each experiment, we generate L independent trajectories from both systems using the same Brownian noise realization. At every time point t_k , this produces two empirical distributions consisting of L samples each. We then compare these distributions using the Kolmogorov–Smirnov statistic and the Wasserstein distance.

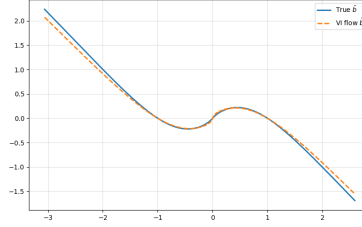


Figure 4: Comparison of the estimated drift and the averaged drift.

Figures 3 show kernel density estimate (KDE) comparisons of the empirical laws at selected time instances for increasing numbers of sample paths L . As L increases, the empirical distributions become more stable and the agreement between the learned averaged dynamics and the true averaged dynamics becomes more apparent.

The comparisons demonstrate that the inferred drift reproduces not only individual sample-path behavior, but also the finite-time probabilistic structure of the averaged system.

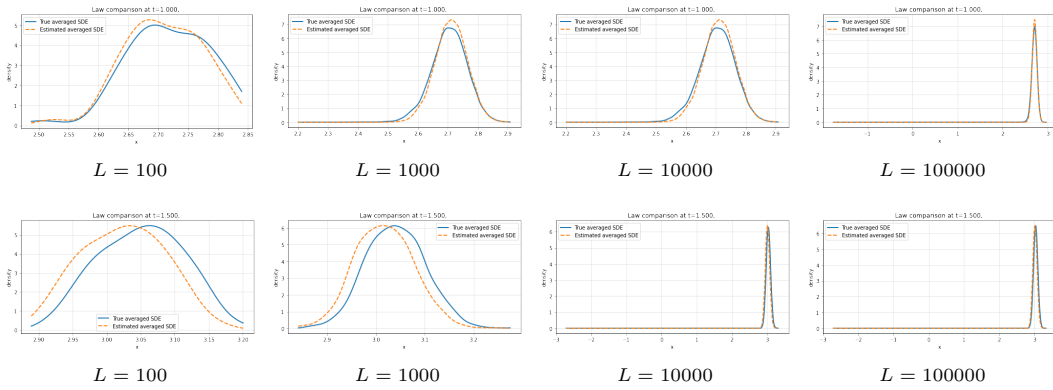


Figure 3: Law comparison at $t = 1$ and $t = 1.5$ for different numbers of sample paths L .

Model :Variant of Double-well dynamics.

Double-well example: We consider a slow–fast SDE system where the fast dynamics evolve with the invariant distribution given by a four-dimensional von Mises law. The slow component satisfies a nonlinear double-well type dynamics with drift

$$b(x, y_1, y_2, y_3, y_4) = \frac{x - x^3}{1 + x^2 + y_1^2 + \sin(1 + y_2^2) + \log(1 + y_3^2) + y_4^4}.$$

The cubic structure in the numerator induces a double-well behavior in the effective averaged dynamics, while the denominator introduces a highly nonlinear dependence on the fast variables.

Experimental Design: Synthetic observations are generated by simulating the corresponding multiscale slow–fast SDE system using Euler–Maruyama discretization over a fixed time horizon. The fast dynamics are simulated independently and subsequently coupled with the slow process through the above interaction drift. The averaged drift is then learned using the proposed variational flow framework.

Comparison: Figure 4 compares the true averaged drift with the estimated averaged drift obtained from the variational normalizing flow model. The learned drift accurately captures both the global double-well structure and the local nonlinear behavior near the origin, demonstrating that the proposed method is capable of recovering complicated averaged dynamics induced by nonlinear fast variables. The attached simulation code can be cited separately if needed.